Advances in Water Resources 44 (2012) 126–139

Contents lists available at SciVerse ScienceDirect

Advances in Water Resources

journal homepage: www.elsevier.com/locate/advwatres

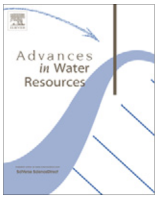

Numerical simulation of DNAPL source zone remediation with *in situ* chemical oxidation (ISCO)

Michael R. West *, Bernard H. Kueper [1]

Queen's University, Kingston, Ontario, Canada K7L 3N6

ARTICLE INFO

Article history:
Received 24 June 2010
Received in revised form 1 May 2012
Accepted 2 May 2012
Available online 17 May 2012

Keywords:
DNAPL
Remediation
ISCO
TCE
PCE
Modeling

ABSTRACT

Numerical simulations were conducted to evaluate the efficacy of *in situ* field scale chemical oxidation (ISCO) (with permanganate) for trichloroethylene (TCE) and tetrachloroethylene (PCE) DNAPL in eight idealized heterogeneous porous media sites. The goal of this work was to study the effects of DNAPL source zone remediation at the site scale utilizing a high-resolution three-dimensional numerical model. The model results demonstrated that both dissolution (no treatment) and treatment were unable to completely deplete DNAPL mass or boundary mass flux for any of the sites over a 10 year period. Performance was highly variable due to competition with oxidizable organic aquifer materials, manganese dioxide (rind) formation, DNAPL architecture, and geologic characteristics. When compared to dissolution only, DNAPL mass depletion at the end of treatment ranged from adverse impacts to a three-fold improvement, but diminished with post-treatment monitoring. Similarly, the relative reduction in boundary mass flux varied between unity and a factor of two at the termination of treatment, but at 10 years ranged from a 10-fold reduction to adverse impacts. During the post-treatment phase of the simulations, most of the benefits achieved during active treatment were negated due to dissolution tailing.

1. Introduction

The benefit of source zone partial mass removal on plume evolution at sites impacted by dense non-aqueous phase liquids (DNAPLs) is a topic of considerable interest in the remediation industry [15,33,41,52,58]. A variety of approaches can be considered for in-situ DNAPL mass removal including hydraulic displacement, chemical flushing, thermal treatment, and enhanced biodegradation. Within the broad class of chemical flushing technologies, much attention has been given to oxidation using permanganate.

The oxidation of trichloroethylene (TCE, C_2Cl_3H) and tetrachloroethylene (PCE, C_2Cl_4) by permanganate (MnO_4^-) are represented as [6,73,75]:

$$C_2Cl_3H + 2MnO_4^- \Rightarrow 3Cl^- + 2CO_2 + H^+ + 2MnO_{2(s)} \tag{1}$$

$$C_2Cl_4 + 2MnO_4^- \Rightarrow 2Cl^- + Cl_2 + 2CO_2 + 2MnO_{2(s)} \tag{2}$$

It is recognized that alternate formulations for stoichiometry have been published for PCE [29,38]. The successful enhancement of TCE and PCE DNAPL mass removal by permanganate has been demonstrated experimentally in the laboratory [38,49,60,61] and at the field scale [60]. However, the effectiveness of treatment is conditional. In (1) and (2) the solid manganese dioxide is a byproduct of the chemical oxidation process. The $MnO_{2(s)}$ is a colloidal particle that can precipitate [10,28], reducing permeability by clogging soil pores [51,61,63] and portions of fractures [65], and forming a low permeability deposition zone (rind) at the DNAPL-aqueous phase interface [67] that can encapsulate DNAPL source zones [9,35,38,61]. The factors that influence the formation and precipitation of $MnO_{2(s)}$ are highly variable and site specific, depending on pH, interstitial pore velocity, contaminant concentration, cation concentration, buffering capacity, and permanganate loading [10,11,32,46].

It has been found that (1) and (2) follow a second-order reaction rate when MnO_4^- is in excess [12,25,27,62,69,73] (first-order in PCE or TCE and first-order in MnO_4^-). Experimentally determined second-order reaction constants for TCE and MnO_4^- (k_{TCE}) have been reported to range between 0.24 and 1.19 $M^{-1}\,s^{-1}$ (for 20–25 °C) [27,69,74]. Similarly, values ranging from 0.028 to 0.051 $M^{-1}\,s^{-1}$ (for 20–25 °C) have been determined for PCE and MnO_4^- reactions [12,25,29,32,69]. This second-order reaction rate follows the Arrhenius equation with respect to temperature, which is useful for estimating reaction rate constants consistent with groundwater temperatures [12,74].

Since MnO_4^- indiscriminately reacts with a multitude of naturally-occurring organic and reduced inorganic compounds, the presence of organic and inorganic species on soil subject to chemical oxidation can result in substantial competition with the targeted

---

* Corresponding author. Tel.: +1 613 533 6834; fax: +1 613 533 2128.
E-mail address: mwest@ce.queensu.ca (M.R. West).

[1] Tel.: +1 613 533 6834; fax: +1 613 533 2128.

0309-1708/$ - see front matter © 2012 Elsevier Ltd. All rights reserved.
http://dx.doi.org/10.1016/j.advwatres.2012.05.001

Notation

a^n	effective interfacial area $\{L^2\,L^{-3}\}$
C	concentration $\{M\,L^{-3}\}$
C_{norm}	normalized mean average concentration or concentration reduction
C_s	effective solubility $\{M\,L^{-3}\}$
d_{50}	mean grain size diameter $\{L\}$
D	hydrodynamic dispersion tensor $\{L^2\,T^{-1}\}$
D^o	free water diffusion coefficient $\{L^2\,T^{-1}\}$
E_m	DNAPL mass enhancement factor
E_f	boundary mass flux enhancement factor
F_{norm}	normalized boundary mass flux or flux reduction
f_{oc}	factor of organic carbon
g	gravitational acceleration $\{L\,T^{-2}\}$
∇h	hydraulic gradient
J	interphase mass flux $\{M\,L^{-3}\,T^{-1}\}$
k	permeability $\{L^2\}$
k_{ij}	intrinsic permeability tensor $\{L^2\}$
k_{la}	average mass transfer coefficient $\{L\,T^{-1}\}$
K_l	lumped mass transfer coefficient $\{T^{-1}\}$
k_o	original permeability $\{L^2\}$
k_{OAM}	reaction coefficient between OAM and MnO_4^- $\{M^{-1}\,L^3\,T^{-1}\}$
K_{oc}	organic carbon partition coefficient
k_{PCE}	reaction coefficient between PCE and MnO_4^- $\{M^{-1}\,L^3\,T^{-1}\}$
k_r	relative permeability {–}
k_{TCE}	reaction coefficient between TCE and MnO_4^- $\{M^{-1}\,L^3\,T^{-1}\}$
M_{DNAPL}	DNAPL mass in domain $\{M\}$
M_f	total boundary mass flux $\{M\,L^{-2}\,T^{-1}\}$
M_{norm}	normalized DNAPL mass or DNAPL mass reduction
P	pressure $\{M\,L^{-1}\,T^{-2}\}$
P_C	capillary pressure $\{M\,L^{-1}\,T^{-2}\}$
q	Darcy flux $\{L\,T^{-1}\}$
q_s	volumetric flux representing sources and/or sinks $\{T^{-1}\}$
R	retardation factor
S	phase saturation
S_E	effective saturation
S_W	wetting phase saturation
S_{rind}	rind function $\{L^2\,L^3\,M^{-1}\}$
t	time $\{T\}$
v	average linear groundwater velocity $\{L\,T^{-1}\}$
x	horizontal longitudinal direction
y	vertical direction
z	horizontal transverse direction
Δx	nodal dimension along x direction $\{L\}$
Δy	nodal dimension along y direction $\{L\}$
Δz	nodal dimension along z direction $\{L\}$
X	dimension of domain along x $\{L\}$
Y	dimension of domain along y $\{L\}$
Z	dimension of domain along z $\{L\}$
α	porous medium compressibility $\{M^{-1}\,L\,T^2\}$
$\alpha_{x,y,z}$	dispersivity $\{L\}$
β	wetting phase compressibility $\{M^{-1}\,L\,T^2\}$
ε_{rel}	relative difference in saturation
Γ	fitting parameter
λ_H	horizontal isotropic correlation length $\{L\}$
λ_V	vertical isotropic correlation length $\{L\}$
μ	dynamic viscosity $\{M\,L^{-1}\,T^{-1}\}$
$\mu_{\ln k}$	mean of ln k $\{\ln(L^2)\}$
ρ	fluid density $\{M\,L^{-3}\}$
$\sigma^2_{\ln k}$	variance of ln k $\{[\ln(L^2)]^2\}$
τ	tortuosity
θ	porosity
$\mathcal{R}$	rate of all reactions $\{M\,L^{-3}\,T^{-1}\}$

Common subscripts

0	initial condition
i, j	coordinate indices for x, y, z
W	wetting phase
NW	non-wetting phase
m	mobile species
im	immobile species

Common superscript

n	species number

chlorinated solvents, yielding reduced treatment efficiency [43,62]. Considering only reactive organic aquifer material (OAM), the reaction between OAM and permanganate can be given by [42]:

$$3CH_2O + 4MnO_4^- \rightarrow 3CO_2 + 4MnO_{2(s)} + H_2O + 4OH^- \tag{3}$$

Eq. (3) represents a reactive sink often referred to as the natural oxidant demand (NOD). The NOD of soil has been experimentally investigated by Mumford [42], Mumford et al. [43], Hønning et al. [24], and Urynowicz et al. [68]. The authors reported that the NOD reaction between OAM and MnO_4^- consisted of independent fast and slow reactions. Mumford [42] modelled the experimental data using two independent second-order kinetic reactions with a reasonable match; Hønning et al. [24] studied NOD for two aquifers finding that 50% of the MnO_4^- is consumed in the fast reaction that occurs within the first 12 h of treatment and followed a first-order reaction rate; Urynowicz et al. [68] derived a rate expression comprising two independent first-order reaction rates solely dependent on $[MnO_4^-]$ that was a good match to their experimental results, with the transition between fast and slow occurring at approximately 48 h.

Field-scale modelling of the *in situ* chemical oxidation of DNAPLs is sparse in the literature. Zhang and Schwartz [75] conducted two simulations: a three-dimensional domain (3 m by 2.5 m by 1 m with 1350 nodes) representing the Borden aquifer test cell experiment conducted by Schnarr et al. [60], and a large scale two-dimensional domain (120 m by 70 m with 2601 nodes) representing a US Department of Energy site. Ibaraki and Schwartz [30] investigated the influence of soil heterogeneity and fluid density-effects on sweep efficiency with a 15 m by 12 m two-dimensional domain comprising 11,640 nodes. Henderson et al. [22] studied the effects of density-dependent flow and geochemistry on ISCO performance for a pilot test within a sheet pile cell measuring 28 m by 32 m by 8.2 m deep, discretized into 29,791 nodes; the modeling simulated two permanganate injections at a well-characterized industrial site impacted with residual TCE DNAPL.

In this study, the three-dimensional two-phase flow reactive transport model, DNAPL3D-RX [70], was modified and utilized to investigate the treatment of TCE and PCE DNAPL source zones in field scale heterogeneous porous media by chemical oxidation with potassium permanganate. Treatment effectiveness was primarily evaluated with respect to DNAPL mass removal and solute mass flux reduction over a simulated period of 10 years in both the presence and absence of treatment. This work focused on the influence of: (i) soil permeability and heterogeneity, (ii) DNAPL